Final Report
Georgia Cancer Coalition (GCC)

Project Title

Development of a label free glycan arrays for the detection of prostate cancer

Georgia Institute of Technology

Principal Investigator:

Ali Adibi
Professor, School of Electrical and Computer Engineering,
Georgia Institute of Technology
Atlanta, GA 30332-0250
e-mail:adibi@ee.gatech.edu
Tel: (404) 385-2738
Fax: (404) 894-4641

April, 2014

Report Summary: This report provides an overview of the collaborative research between the Dr. Ali Adibi from Georgia Institute of Technology and Dr. Richard Cummings from Emory University for development of label-free Glycan arrays that can be used toward the detection of cancer specific biomarkers for different cancers, specifically alternative biomarkers for prostate cancers. The goal of this program was to develop initial proof of concepts for glycan arrays to promote larger size program from Federal funding agencies. The proposed microarray or multiplexed sensing platform is based on an array of compact resonators each coated with a different molecular probe that can target different set of glycan binding protein (i.e., lectin) biomarkers. During this program, Adibi and Cumming groups worked closely to demonstrate multiplexed sensing platform based on array of compact resonators coated with different set of glycan surface coatings. To achieve this, during this project several important challenges from the design of the sensor array and developing of the surface functionalization protocols to the design of optimal microfluidic channel and development of optimal technique for accurate measurement of the resonators resonance wavelength shift have been addressed. The outcome of this one-year project sets the stage for the future work for cancer biomarker discovery and cancer detection device and systems. Adibi and Cummings are working closely to apply these results and finding of this project in new problems and have submitted several joint proposal to the federal funding agencies (especially NIH) including one for development of a new technique for prostate cancer detection based on identification of the glycan group of the prostate specific antigen (PSA) using the developed multiplexed sensing platform.

Introduction: Prostate cancer is one the most commonly diagnosed cancers in males in the United States and ranks second among tumor site-specific mortality, with estimates for 2009 at over 192,000 new cases and 27,000 deaths [1]. A major advance in screening for prostate cancer was the identification of the prostate specific antigen (PSA), a biomarker test that has resulted in an increased incidence of diagnosed prostate cancer. While the PSA test is widely used and is quite sensitive, it is not highly specific and there is an unmet and very important need to develop new biomarkers for more accurately discriminating prostate cancer from benign disease states. Moreover, there is also growing evidence that tumor cells in general exhibit altered glycosylation of surface glycoproteins and glycolipids in the so-called glycocalyx [2]. These altered molecules released from tumors may be immunogenic and stimulate T- and B-cell dependent immune responses with the development of anti-glycan antibodies. Such anti-glycan antibodies generated against tumors afford a novel biomarker opportunity for study. However, a major challenge that has stymied the development of such anti-glycan antibody assays is the lack of suitable highly sensitive and robust strategies for detecting such tumor-specific anti-glycan antibodies. Glycan microarrays based on a secondary fluorescent label are currently being used for many applications; however, they require finding an appropriate label that functions uniformly with all of the desired antibodies. This is especially difficult in this case as the target autoantibody is not known before the detection. Label-free glycan microarrays resolve this issue as they do not require any secondary labeling.

The main goal of this work is to develop a label-free glycan microarray based on a densely multiplexed array of refractive index sensors. Such glycan microarray enable to detect the main autoantibodies that are produced by humans for the cancer specific glycan antigens. Once unique glycan antigens are identified, they may be used to generate specific monoclonal antibodies to tumor cell glycans that will be useful in targeting therapeutics to the tumors.

Our main focus in this project has been on developing a label-free resonance-enhanced glycan-functionalized microarray or multiplexed sensing platform and optimization of the performance and sensitivity of it. To achieve this, several different tasks have been done to 1) develop a multiplexed sensing platform based on a resonator array, 2) develop the required surface chemistry for binding of the glycan surface coating to the surface of the sensing elements, 3) design and implement the required sample delivery system to optimize the input analyte interaction with the sensing elements, 4) development of accurate resonance wavelength shift measurement to achieve high sensing sensitivity, and 5) testing of the developed sample for different target analyte to demonstrate the overall performance of the system. Furthermore, we have developed different techniques to improve the sensitivity of the developed sensing platform based on developing sensors with porous surface and integrating the developed sensor array with microfluidic systems for sample pre-concentration. This report provide a summary and high-light of the research done under this project.

1) Development of a multiplexed label-free microarray

1.1) Introduction: A resonator-based refractive index sensor is a label-free sensor that detects the target analytes by monitoring the changes in the resonance wavelength of the resonator, caused by the analyte binding to the resonator surface. High-Q resonators provide high sensitivity to the changes in the refractive index of their surrounding environment, as a small shift in their resonance wavelength leads to a considerable change in their transmission characteristics, at wavelengths close to their resonance wavelength. A resonant-based refractive index sensor in its simplest form is a waveguide-coupled resonator or a Mach-Zehnder (MZ) interferometer with a resonator coupled to one or both its arms. Figure 1 shows the schematic of a resonator-based refractive index sensor. The shift in the resonance wavelength manifests itself in the changes in the transmission of the sensor device and can be estimated by measuring the changes in the device transmission at a certain wavelength or over a range of wavelengths.

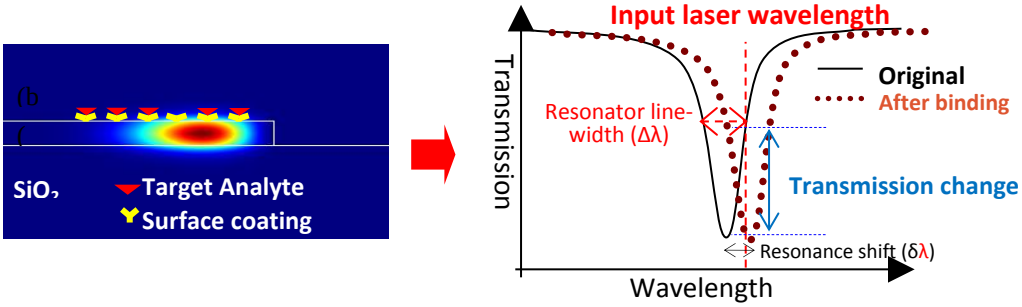

Figure 1: Schematic of the refractive index sensing by measurement of the resonance shift of a resonator caused by the analyte binding to the resonator surface. By biasing the input laser at a wavelength with maximum transmission slope, a small shift in the resonance wavelength of the high-Q resonator translates to a large change in the transmission amplitude.

1.2) Multiplexed sensing: A highly-multiplexed refractive index sensor can be implemented by integrating a large number of ultra-compact resonator-based sensors on the same chip. This multiplexing can be done either in the spectral or in the spatial domain. In spectral domain multiplexing, many resonators, each with a different resonance wavelength, are coupled to the same input waveguide to form a resonator array (see Figure 2). The resonant wavelength of each resonator is adjusted by engineering its geometry (i.e., inner and outer radii). Each resonator is coated with a different surface coating to most specifically detect a certain analyte. Each individual resonator in the array can be interrogated independently by monitoring the transmission through the waveguide at the wavelength range corresponding to the resonance of the desired resonator.

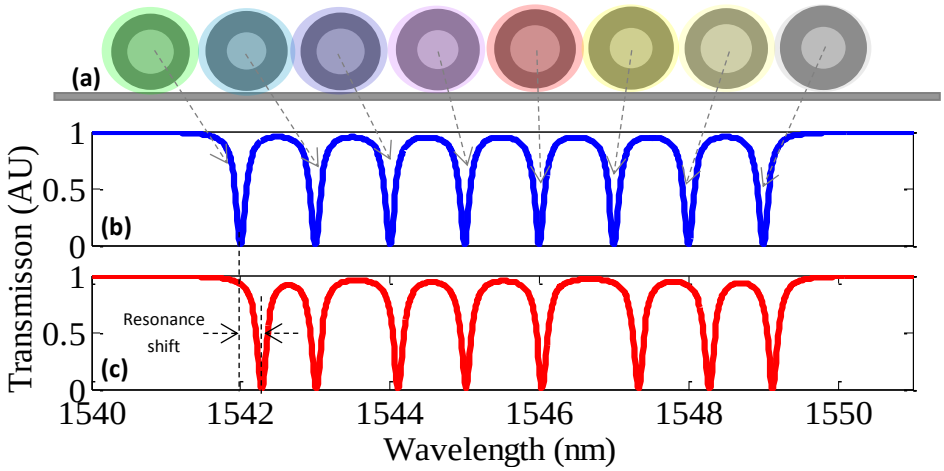

Figure 2: (a) Schematic of a multiplexed refractive index sensor composed of several different resonators, each at a different resonance wavelength, coupled to a common bus (or interrogating) waveguide. The resonance wavelength of each resonator is adjusted by engineering its geometry (i.e., inner and outer radii). Each resonator is coated with a different surface coating to specifically detect a certain analyte. (b) and (c) show the transmission spectrum of the resonator array before and after exposing to the target input sample. Different resonance shifts of different resonators indicate the different degree of binding to analytes in the input sample.

In the spatial domain multiplexing, an array of separate waveguide-coupled resonators is used. The resonator in this case can be designed to have similar resonance wavelengths. In this case, to interrogate each sensor, the output signal of its corresponding waveguide should be measured. The main advantage of the spectral domain multiplexing is that all sensing elements can be interrogated using a single pair of input and output. However, the maximum number of sensing elements that can be multiplexed in the spectral domain is limited by two important factors: 1) the minimal required resonance wavelength shift of each resonator for successful binding detection, and 2) the maximum free-spectral range (FSR) of the resonators in the array, which limits the overall operation bandwidth. Adibi's group has demonstrated

the miniaturized microdisk resonators with world-record performance in silicon on isolator (SOI) platform. These resonators combine a large single-mode FSR and a high Q that is optimum for a large multiplexing degree. For example, using microdisk resonators with a radius of 2μm and a FSR of ~ 54 nm, and assuming a maximum required resonance wavelength-shift dynamic range of 600 pm for each sensor element, up to 90 different sensors (or resonators with proper surface coating) can be multiplexed and coupled to the same waveguide. A larger multiplexing degree can be obtained by combining spectral and spatial multiplexing (e.g., an array of waveguides each coupled to an array of resonators.

1.3) Development of the microarray on SiN on oxide platform:

While the high refractive index contrast of Si in respect to oxide enables to achieve very compact resonators wit h very large FSR, silicon nitride (SiN) material platform provides certain advantages including the much lower temperature sensitivity due to smaller thermo-optic coefficient, higher power handling due to lack of two-photon-absorption and smaller third-order nonlinearity, and low absorption at visible and NIR wavelengths that enables to implement the microarray at visible wavelength where we get much lower water absorption and we can multiplex the refractive index sensing with other modalities such as fluorescent and Raman sensing. Therefore, we have focus most of our efforts on developing the microarray on SiN platform. While SiN due to its smaller refractive index may not provide FSRs as high as those that can be achieved by SOI platform, a combination of spatial and spectral multiplexing can be used to compensate for this. The availability of chip high quality detector arrays and CCDs at visible and NIR wavelengths enables to implement low cost microarrays based on CCD detectors. Figure 3 demonstrates as example of fabricated microarray on SiN platform. The devices has been fabricated and processed at Georgia Institute of Technology's cleanroom facility. Cleaved pieces of the wafer are cleaned by acetone, methanol, and isopropanol rinse. The chips are dehydrated for five minutes of at 100C on hotplate and spin coated after cooling. ZEP520A is spun at 1500 RPM for 1 minute, and then baked at 180C for two minutes. Coated chips can be kept in a dark place for a few weeks. Right before electron beam lithography (EBL), ESPACER was spin coated at 4000 RPM for 30 seconds on the pieces, to reduce charge-up effect. Device patterns are written using JEOL JBX-9300FS EBL System into ZEP, with a current of 2 nA and dosage of 200 μ C/cm 2. Before developing, the chips are rinsed with running deionized (DI) water for 1 minute to wash the ESPACER layer. Next they are developed in amyl acetate for 2 minutes with gentle agitation, and then soaked in isopropanol for 30 seconds. Dried chips are etched in Oxford endpoint RIE etcher using CF 4 plasma (20 sccm CF 4 flow, 200 W power, 10 mTorr pressure). Residual ZEP is removed after the etch by soaking the chips in Microposit remover 1165 at 80C for 20 minutes, followed by acetone rinse. The chips are cleaned in Piranha (5:1 H 2 SO 4 and H_2O_2) for 10 minutes and then rinsed with DI water.
Figure 3.a shows the layout of the developed SiN multiplexed resonator array, Figure 3.b shows the schematic of the resonators in each row showing the sensing and reference (Coated by SU8) resonator, and Figure 3.c shows the top microscope image of the fabricated sample with opening in cladding SU8 material for sensing elements. In this sample on each row we have provided two reference and three reference resonators that can be coated with different glycans. A large number of sensing element can be achieved by using multiple sensing lines (Figure 3.a).

To characterize the fabricated sensors, the transmission spectra of the fabricated resonator array is measured. Focused laser light is side-coupled to the waveguides at the edge of chip. Laser source is a New Focus TLB 6305 tunable laser module sweeping 652-660 nm window. Laser's output is conditioned by a half-wave plate and a polarizing beam splitter to rotate the polarization of the laser output onto TM direction and suppress the TE component. The device is aligned to have the edge of the input waveguide in the focused laser beam. On the other end, another lens is used to project the output light onto a silicon detector. Collected spectral data is analyzed for detecting the resonances and fitting a Lorentzian to the detected resonances. Figure 4 shows the schematic of the transmission spectra of the

resonators on one of the rows at wavelengths between 650 nm to 660 nm measured by using a detector that collects the light from collected by a top detector. Each peak at this image corresponds to one of the resonance wavelength of one of the reference or sensing resonator. Therefore the binding to the resonator surface can be detected by monitoring the shift on the resonance wavelength of these resonators.

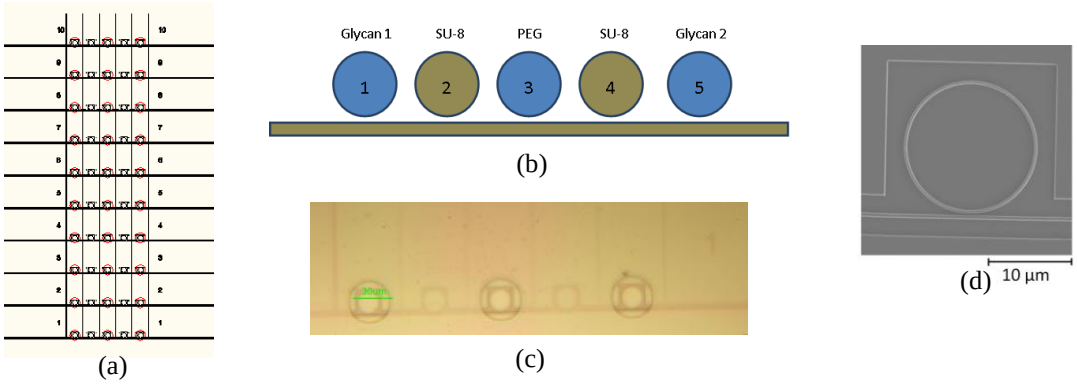

Figure 3: The schematic of a developed SiN multiplexed resonator array. (a) The designed lay out of the sensor array. (b) The schematic of the resonators in each row showing the sensing and reference (Coated by SU8) resonator. (c) The top microscope image of the fabricated sample with opening in cladding SU8 material for sensing elements. (d) SEM image of one of the resonators in the array.

2) Development of surface chemistry protocols for the glycan microarray

After the development of the surface of the sensing elements are coated by different glycan surface coating. In order to increase sensitivity and also specificity of photonic sensors, we modify the surface of the sensor by grafting cognate receptor of target ligands. This surface modification is slated to capture target cells or molecules and thus considerably enhance the sensitivity by increasing the density of target on the surface. Also this surface chemistry is designed to suppress non-specific binding of competing targets to the surface, which boosts the specificity of the sensor. Glycans provide a viable platform for sensing, as they provide a wide range of receptors that can distinguish between many different targets (e.g. toxins) using a panel of glycans in the form of microarray [3]. In our scheme, we immobilize glycans on the sensor microarray, and detect binding of target anaylte using the sensing platform. Employed glycans are derivatized to include amine moiety on their surface. Thus by grafting carboxylate group on the sensor surface glycans can be fixed on the surface using a strong peptide bond. First step of this surface chemistry on silicon, silicon dioxide, or silicon nitride starts with alkoxysilane end-group in order to graft a self-assembled monolayer on the surface. Most conventional procedure is grafting of 3-aminopropyltriethoxysilane (APTES) which provides amino group, and then application of NHS-EDC chemistry to the Si-APTES surface [4]. In order to suppress non-specific binding it is customary to PEGylate the surface by incorporating poly(ethylene

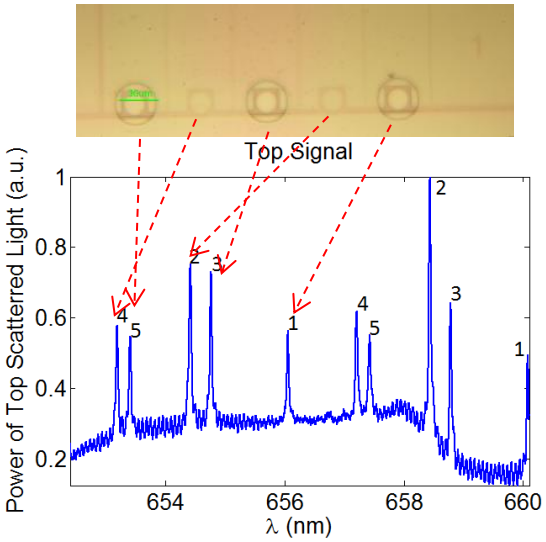

Figure 4: The characterization results of the resonator array in SiN platform. Different peaks correspond to different sensing and reference resonators in the array.

glycol) chains under receptor layer. In above mentioned chemistry this can be done by using PEG bearing amine-amine linker, like Bis(succinimidyl) nona(ethylene glycol), instead of NHS-EDC chemistry. Tween-20 [5] and BSA [6] has also been used for prevention of non-specific binding. Finally we immobilize our glycans by incubating them on aminated substrate.

We start by degreasing and cleaning the substrate by rinsing the sample using acetone, methanol and isopropyl alcohol. Next sample is soaked in Piranha solution (3:1 H2SO4, 30% H2O2) for 15 minutes, for cleaning and activation of hydroxyl groups on the surface. Then sample is immersed in 1%w/v silane-PEG-NHS [7] (Figure 5) in dry DMSO, for 5 hours at room temperature. Afterwards sample is rinsed with dry DMSO and dried using nitrogen blow. At this stage sample is PEGylated and aminated. Glycans are then spotted on specific locations and sample is incubated at 50C for one hour. When incubation is done, the sample is let dried and washed in PBS with 0.05% tween-20 and then is washed in ddH2O. Blocking is done by immersion in 50mM ethanolamine in 50 mM sodium borate (pH 8.0) for 1 hour. Afterwards same washing protocol is applied to remove any chemical residues.

To evaluate the performance of the developed surface coating protocol for the SiN surface, we first performed the process to coat the surface of a SiN sample with a few different glycan and test the binding with different lectins. Figure 6 shows that fluorescent image of the binding between different fluorescent tagged lectins and different glycan surface coating and the binding strength can be evaluated by measuring the emitted fluorescent signal. The binding strength in this case matches with the expectations and this verifies the reliability of the developed surface coating process.

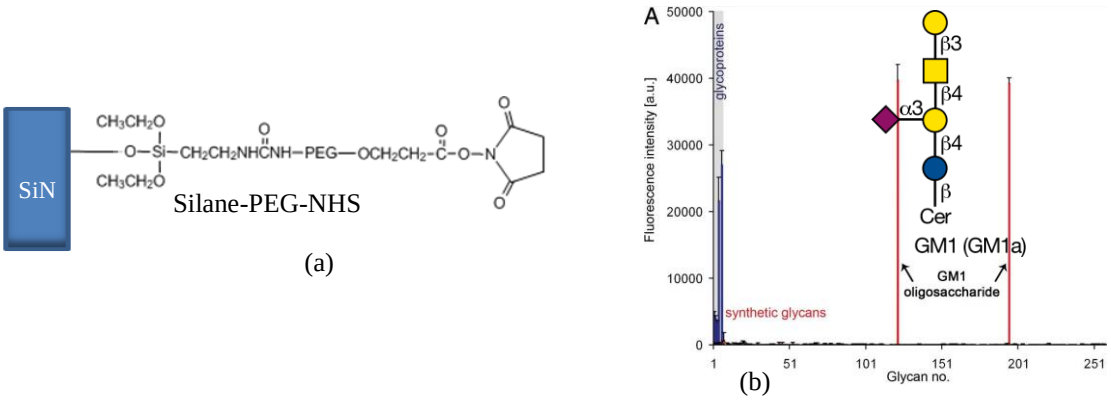

Figure 5: (a) Schematic of binding PEG and NHs to SiN surface using single step process using Silane-PEG-NHS molecule(b) Examples of the binging Specificity for the protein on a virus surface: Simian Virus 40.

We then used the same surface coating process to coat the surface of different resonator in the developed resonator array. We have used different physical methods for applying the coatings to the small area transducer surfaces using the deposition tools available at the Georgia Tech NRC. The Nano eNabler (Bioforce Nano) is a multifunctional surface patterning tool that can be used for precise selective coating of the sensor surface. It enables dispensing attoliter to femtoliter volumes of biomolecules, nanoparticles and other liquids onto a wide variety of surfaces. Using a grooved cantilever surface patterning tool, we have been able to pattern drop sizes with down to 3 μm diameter with very high alignment accuracy. Alternatively, ink-jet printing (Microfab jetlab II) can produce drop-on-demand as small as 10 μm diameter.

After the coating of the resonator surface, the binding kinetic between the surface coating glycan and the lectins can be measured using the developed label-free refractive index sensor. Figure 7 shows the changes in the resonance wavelength of the resonator versus time, caused by the binding of the ConA molecules to the resonator surface coated by Man5 Glycan. A maximum shift of 30 pm is observed for the addition of 20 uL of a streptavidin solution with a concentration of 10μg/mL in a reservoir, already filled with 20 uL of buffer solution on top of the sensing resonator. Because of the high concentration of the ConA solution in this experiment, we expect that all the binding sites on the sensor surface are filled with conA molecules.

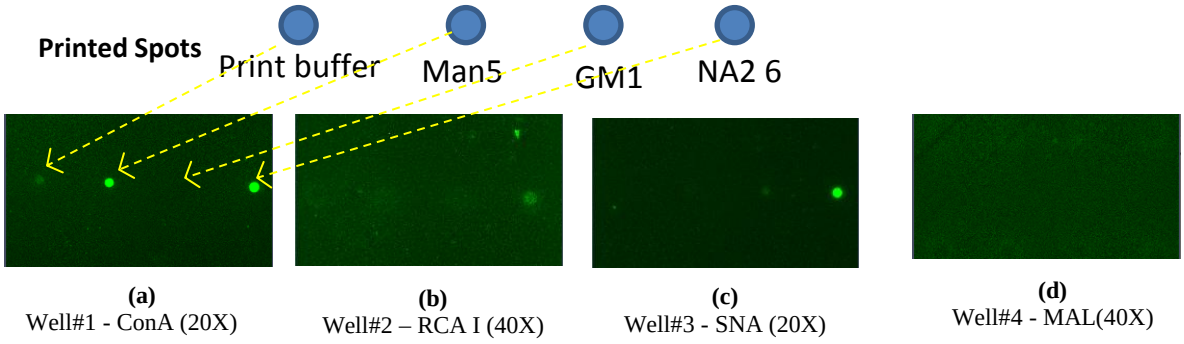

Figure 6: (a) The test of the surface binding of different lectins to the coated glycans using the dev eloped surface chemistry on the SiN surface.

3) Development of Multiplexed Sensing Platform

To study the performance of the sensor for the detection of a mixture of proteins, we have used 3FL and 2,6-NA2 glycans as surface receptors, to detect and quantify the concentration of Aleuria Aurantia Lectin (AAL) and Sambucus nigra lectin (SNA). Each glycan/protein pair is tested individually at first, in order to estimate the binding dynamics of the pair. This test is carried out by immobilizing one glycan on three sensing rings, while leaving the other three sensing rings un-coated (i.e., having only the PEG brush). The corresponding protein with various concentration is applied to the sensor the dissociation constant (K_D) is measured from the dose-response curve. In the next test, each of the two glycans are immobilized on two different sensing rings, leaving the remaining two microrings (out of six) un-coated. Two mixtures of these two proteins are prepared (a low-concentration and a high concentration mixture), and applied to the sensor sequentially.

We use the high concentration phase to calculate the saturation response (R_0) as: ($R_0 = R_H (C_H+KD)/ C_H$), where R_H is the high concentration response (defined as the shift at the end of high concentration phase), C_H is the high concentration of the lectin being studied, and KD is the dissociation constant of the glylcan/lectin pair being studies. Subsequently, the concentration of the low-concentration phase is estimated using, $C = R_0 C_L/(C_L+KD)$. Figure 8.a shows The result of multiplexed sensing of the two proteins. The experiment is repeated on two similarly prepared sensor chips. Resonance shift of the ring sensors with 3FL (blue) and 2,6-NA2 (green) glycans coating to low-concentration (CL) and high-concentration (CH) mixtures.

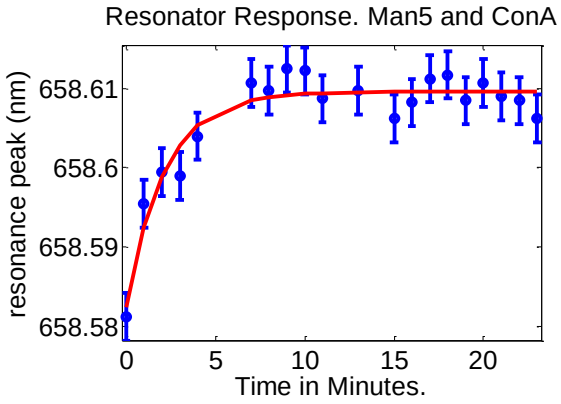

Figure 7: The characterization results of the resonator array in SiN platform. Different peaks correspond to different sensing and reference resonators in the array.

4) Development of more efficient technique for the measurement of the resonance shift

The perturbation of resonance caused by biological or chemical molecules at the vicinity of a resonator has proven to be a sensitive trnasduction mechanism for lab-on-chip sensors [8,9]. For an individual on-chip resonator with a linear response, the limit of detection (LOD) is defined as, $LOD = 3\sigma/S$, where S is the sensitivity, and σ is the standard deviation of

output fluctuations (resonance shift here) for blank input. Smaller LODs are achieved either by the enhancement of device sensitivity (S), or through the improvement of detection accuracy (by reducing 3σ). Although an increase in device sensitivity can compromise other system performance measures, such as multiplexing capability within a fixed wavelength window, an improvement in the detection accuracy does not cause such compromises. Improving this accuracy in applications relying on highly multiplexed arrays entails maintaining a homogeneous performance across a wide bandwidth of scan. In this sense, although for small dynamic ranges high accuracies may be readily achieved by simple interrogation systems, the same system does not necessarily help highly multiplexed systems scanning a wide window of wavelength. We have developed a new interferometric referencing method that remarkably suppresses wavelength noise, and thus improves the resonance detection accuracy across an 8 nm window of scan. No temperature control is used, and by taking the advantage of sub-periodic interferometric data an improvement by more than one order of magnitude is realized. Next section presents the device, the interferometric referencing method, and the experimental results.

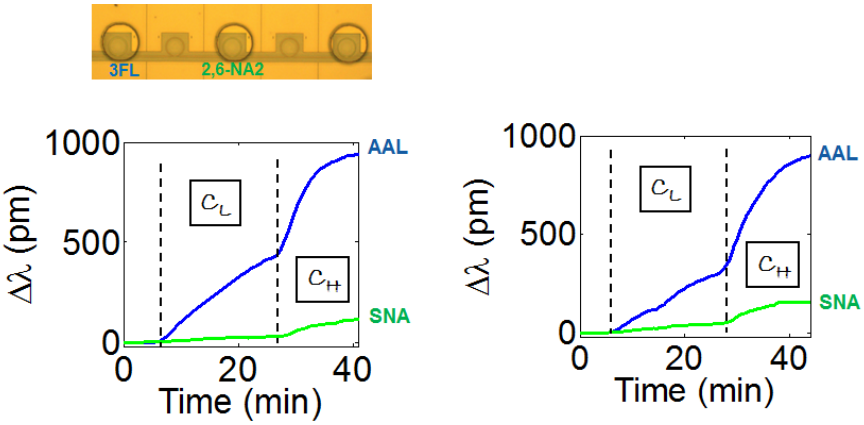

Figure 8, The result of multiplexed sensing of the two proteins. The experiment is repeated on two similarly prepared sensor chips. Resonance shift of the ring sensors with 3FL (blue) and 2,6-NA2 (green) glycans coating to low-concentration (C_L) and high-concentration (C_H) mixtures.

We have employed silicon nitride microring resonators on a silicon dioxide substrate, working at visible wavelength [10]. Five such microrings with a width of 500 nm and an outer radius of 20 mm (FSR = 1.65 nm) are coupled to a common bus waveguide as illustrated in Figure 9 (a). The laser light is coupled to the waveguide at the edge of the chip and the intensity of output light is recorded using a silicon detector. A NewFocus external cavity diode laser (linewidth < 300kHz) is used for scanning the wavelength in 652-660 nm window, as illustrated in Figure 9 (c). A sample of the recorded spectrum is demonstrated in Figure 9(b).

In order to compensate for temperature variations, and also laser wavelength drifts from one scan to the next, we measure the resonance shifts differentially (i.e., subtract the detected resonance of a second microring from that of the microring intended for sensing). We consider 20 resonances in the 8 nm window of scan for our study here (four azimuthal modes of each microring). For an undisturbed setup, the standard deviation of differential resonance shifts, calculated from 60 consecutive scans of the spectrum, is σ = 585 fm.

One potential source of these variations in the detected resonance is the amplitude noise of the transmission signal detected at the detector. Thermal and shot noises, either on the laser output or at the detector, contribute to this noise. Furthermore, we have observed electrical interferences, and mechanical vibrations at coupling points, to affect the signal-to-noise ratio (SNR). The amplitude noise or reasonable

thermal variations, as it will be discussed in this talk, cannot cause the above mentioned variations in the detected resonance.

Beside the amplitude noises, the inaccuracy of the tunable laser in setting the wavelength introduces an independent source of noise. In order to accurately measure the wavelength and correct such wavelength deviations, we used a free-space Michelson interferometer, depicted in Figure 9 (c).

The scan of the 8 nm window is repeated 60 times, and two detection algorithms, with and without using the interferometer data, are compared on this data set. In the detection method without the interferometer, the wavelength is assumed to change linearly across the scan window. So the sampling times are linearly scaled to calculate the wave-length at each sampling point. However, in the detection method using the interferometer we correct the wavelength for each data point based on the interferometer recording. After extracting the wavelengths, a second order polynomial is fit to 200 data points around the minimum point of the transmission (sampling rate is 20 fm). For the SNR of this setup, this second order fit suffices, compared to more complex fits such as Lorentzian.

We have demonstrated the probability distribution function constructed from one of the pairs in Figure 10(a). This representative figure demonstrates how the application of the interferometric correction suppresses the variations. The statistical analysis for all resonance pairs (excluding same microring pairs) results in σ_{avg} = 41 fm using the interferometer, which shows more than one order of magnitude improvement compared to σ_{avg} = 585 fm without the interferometer, as illustrated in Figure 10(b).

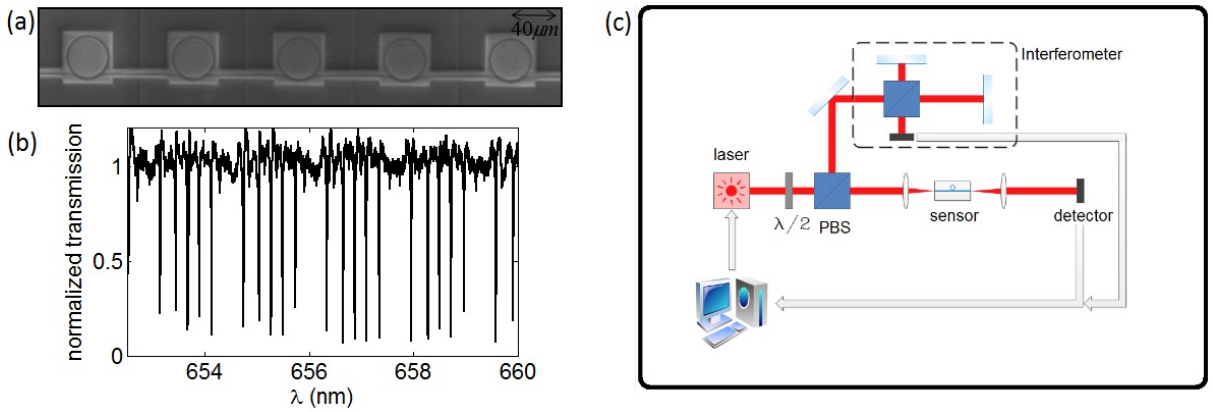

Figure 9. (a) The SEM of the microring. (b) A sample of the measured spectrum. (c) The schematic of the characterization setup.

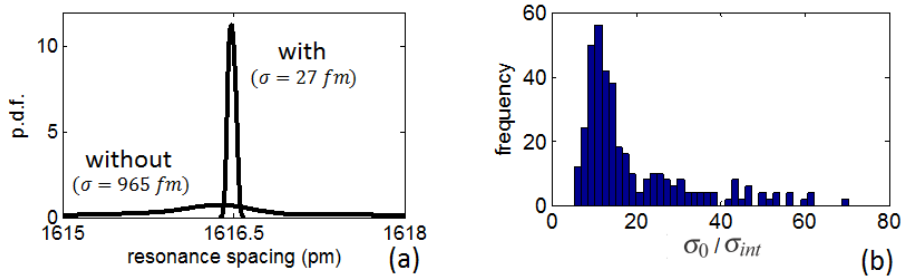

Figure 10. (a) Measured probability distribution function of detected resonance shifts with and without the interferometric referencing. (b) The histogram of the improvement ratio. σ_0 is the standard deviation without interferometer, and σ_{int} is that with the interferometer data; first calculated for each resonance pair and then entered to the histogram.

5) Development of porous-cladding sensing platforms

To increase the sensitivity of the proposed sensors, we fabricate a thin layer of porous material on top of the resonators (porous Si on top of Si devices and porous TiO_2 on top of SiN devices). Figure 11 shows examples of a micro-resonators with a porous Si and TiO2 cladding, fabricated in Adibi's group.

The highly controlled thin porous Si is fabricated by converting a thin layer of oxide to porous Si based on magnesium reduction of oxygen in SiO_2 [11]. The thin porous TiO_2 layer is fabricated using sol-gel technique using sacrificial protamine-carboxyl spheres to control the pores size [12, 13]. The advantage of the proposed techniques over conventional porous structures [14,15,16] is the possibility of achieving a large effective surface area for sensing while maintaining high Q in compact resonators to achieve orders of magnitude higher sensitivity with a very compact device. Our experiments show an enhancement factor of six and ten for the sensors with porous Si and porous TiO_2 claddings corresponding to mass sensitivities of 0.06 pg/mm^2 and 0.016 pg/mm^2 (assuming a resonance wavelength sensitivity of 0.04 pm), respectively. (See Figure 11).

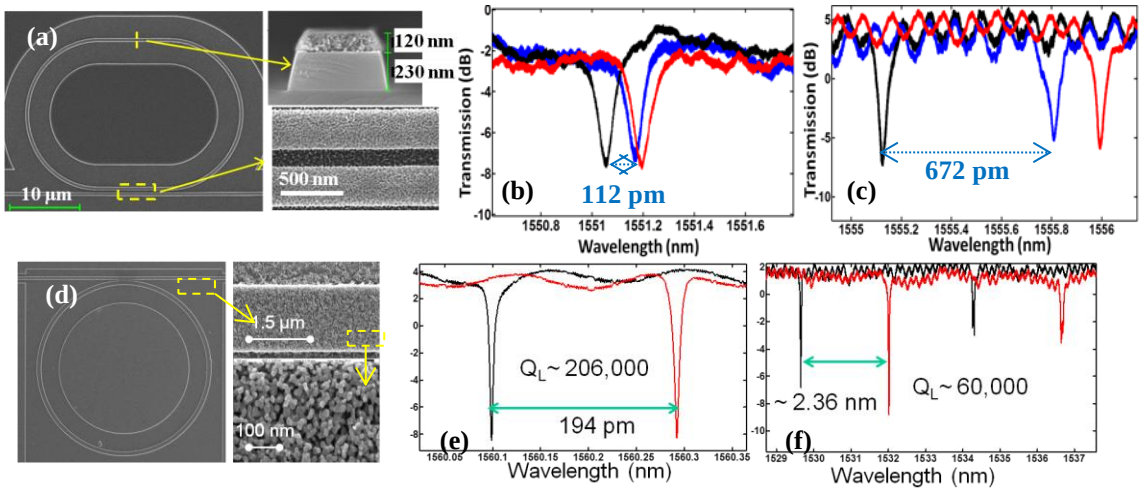

Figure 11, (a) SEM of a racetrack resonator with porous silicon cladding; (insets) close-up image and cross-section images shows uniform porous silicon layer with pore size of 20~30 nm. (b, c) Comparison of resonance wavelength drifts after surface coating with APTES (blue) and Biotin (red). The black curve show the original resonance spectrum. (b) Reference SOI resonators; (c) Porous silicon resonators. A factor 6 improvement in resonance wavelength shift is observed (672 pm for porous sample as compared to 112 pm for .the sample without cladding. The measurement are done for dried samples. (d) SEM of a SiN microring resonator with porous TiO_2 cladding, (e) and (f) the resonance shift with APTES coating for microring resonator without and with porous cladding, respectively. The porous TiO2-cladd sensor demonstrates more than one order of magnitude enhancement in shift selectivity with a high Q of 60 k.

6) New approached for the analysis of PSA

While the main goal of this program has been to develop glycan microarray for detecting new biomarkers for prostate cancer in blood, we have also looked at possibility of looking at structure of PSA itself (rather than only its concentration) as a specific biomarker for prostate cancer. Adibi an dcumming group so have been working actively on developing new approaches for detecting prostage cancer and submitting proposals for federal funding agencies based on this ideas.

PSA is a small 33kDa heavily glycosylated glycoprotein (~8% carbohydrate by weight) [17], but contains a single Asn-glycosylation (N-glycan) site [18] that presents heterogeneous “glycoforms” [19,20,21,22,23,24]. Several recent studies have focused on studying these various glycoforms of PSA as a biomarker for prostate cancer. Such studies demonstrate that there are different glycoforms present that have varying amounts of fucose, N-acetylgalactosamine, sialic acid, and altered and often increased N-glycan branching. Furthermore, analysis of glycoforms of PSA from normal and from the prostate cell line LNCaP revealed major differences in their glycan structures, reflecting the changes in glycosylation pattern that usually take place on the tumor cells [25, 26]. Therefore, we hypothesize that the expressed

and different glycoforms of PSA in serum represent a novel biomarker that can distinguish benign from malignant PCa and may reflect on the stage of the cancer.

Currently, the typical laboratory test for PSA measure the free and/or total PSA using a Immunochemiluminometric Assay (ICMA). This approach cannot identify the glycoforms of PSA, which currently can only be indirectly studied using mass spectroscopy (MS). However, isolation and detailed chemical characterization of PSA from patient serum using MS and other available techniques are impractical, and do not identify the specific glycoforms structure, only size, and in any case are not accessible to common laboratory practices, given the extremely low amounts of PSA in circulation (ng/mL) and the need to analyze so many different samples to allow firm conclusions to be drawn from both quantitative and qualitative data.

Therefore, we believe that it is possible to develop a new low-cost molecular analysis technique for the identification and quantification of different PSA glycoforms. This technique will provide a very high level of sensitivity (LOD ~ 10 pg/mL) with an easy-to-use and rapid assay process that requires very small volumes of input sample (i.e., a few μL). This technique is label-free and allows a definitive test of our hypothesis by identifying and measuring different glycoforms of serum PSA and defining their correlation with the presence and stage of PCa and discrimination of BPH from PCa.

This proposed biomarker screening technique is based on the same developed multiplexed sensing platform developed in this project. However, here we use a two -step process to: 1) filtered and pre-concentrated by capturing it on an anti-PSA functionalized surface; and 2) the captured, and eluted PSA is screened for specific glycoforms both quantitatively and qualitatively using a specialized lectin- and anti-glycan-based microarray (Figure 12). We will prepare PSA glycoforms as standards in which the N-glycans have a wide variety of glycan structures of the types reported by Tabares et al (2006) [27,28,29]. However, the chemical quantities of PSA in human serum are below the limit required for detailed N-glycan sequence analyses, so little is known about all the types of N-glycans present and primarily indirect methods are used [30].

The possibility of screening a large panel of PSA glycoforms provide a large amount of useful information that can be used to develop clinical methods for early detection of prostate cancer as well as diagnosis/monitoring of the prostate cancer stage/progress. Therefore, we are looking toward the demonstration of the performance of the proposed device for accurate and reliable quantification of concentration of different PSA glycoforms using a series of controlled test samples and a limited number of de-identified samples from patients with PCa and PBH. Such device and screening technology enables new extensive clinical studies on the use of PSA glycoform information for patient diagnosis.

Figure 13 shows the schematic of the proposed microfluidic chip for the screening of the PSA glycoforms. In the first step, the PSA molecules are separated from the serum through affinity binding to the PSA antibody immobilized on the surface of a microfluidic channel or on the surface of microspheres trapped in the microfluidic channel (step 1a). The microfluidic channel is then washed with a buffer solution to clean the channel form the traces of the undesired analytes in serum and to wash the nonspecifically bound molecules to the surface. In the second step, the collected PSA molecules are eluted from the antibody-coated surface, and the PSA

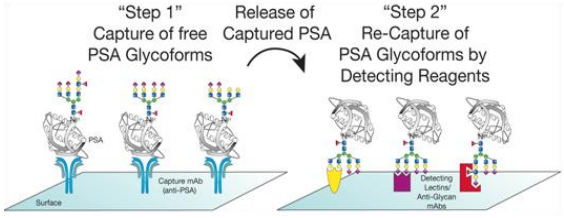

Figure 12, The principal of the identifying and quantifying free PSA glycoforms as biomarkers for benign versus malignant prostate cancer. In step 1, anti-PSA antibodies are used to capture and concentrate free PSA from a serum sample. After washing, the captured PSA is released for Step 2, where its different glycoforms are captured by different detecting regents (antibodies and lectins).

glycoforms is screened by measuring the binding pattern of PSA molecules to a panel of lectins and antiglycan antibodies, carefully selected to distinguish different target glycoforms and immobilized on top of an on-chip photonic resonator array. This process also allows for pre-concentration of the PSA by a relatively large factor (e.g., x100) and considerably enhances the overall detection sensitivity.

A compact, sensitive, and highly multiplexed array of SiN resonators (similar to those developed in this project) can be used for label-free quantification of different PSA glycoform concentrations by measuring their resonance shift due to the binding of PSA to their surface. The SiN chip is integrated with the microfluidic system, which is fabricated using PDMS or glass. The chip will be pre-filled with all required buffers. The assay process will be controlled using pressure-driven flow control, and the integrated photonic microarray will be characterized by using an off-chip tunable laser and a detector array that are optically coupled to the chip through grating couplers on chip. The sample filtering and pre-concentration and the sensing microarray will be separately realized and tested to achieve the target performance; and then they will be integrated to form the complete screening system. We will also develop data processing and analysis tools that provide the concentration of different PSA glycoforms from the raw measurements. The sensing system will be calibrated using a series of controlled pure PSA and serum samples with known concentration of different PSA glycoforms.

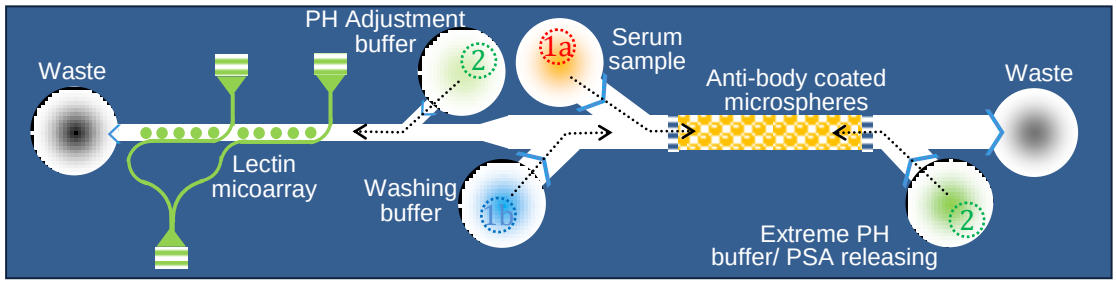

Figure 13, Schematic of the proposed microfluidic chip for PSA filtering and pre-concentration. The fluidic chips is integrated with a lectin/antibody-coated photonic resonator array for the PSA glycoforms screening.

7) Conclusions and Futures works:

Our main focus in this project has been on the demonstration of the label-free microarray. We furthermore, developed different techniques to improve the sensitivity of the developed label-free multiplexed sensing platform to achieve sensitivities needed for the target application in prostate cancer detection. In this program, the Adibi and Cumming groups work closely to develop surface chemistry for functionalization of sensors surface using glycans. The test of this sensing platform has been done with different available lectins that should provide similar binding kinetics to the ultimate target biomarkers. While we are continuing working on the improvement of the developed glycan-based multiplexed sensing platform (i.e., microarray), the Emory and Georgia-Tech team has also worked closely to develop new techniques for prostate cancer detection approach based on glycan and lectin array technology. The work has led to several publications and conference presentations. Here a brief list of the published work through this program.

Publications:

1. Ghasemi, Farshid, Ali A. Eftekhar, David S. Gottfried, Xuezheng Song, Richard D. Cummings, and Ali Adibi. "Self-referenced silicon nitride array microring biosensor for toxin detection using glycans at visible wavelength." In *SPIE BiOS*, pp. 85940A-85940A. International Society for Optics and Photonics, 2013.
2. Xia, Zhixuan, Stan C. Davis, Ali A. Eftekhar, Ari S. Gordin, Murtaza Askari, Qing Li, Farshid Ghasemi, Kenneth H. Sandhage, and Ali Adibi. "Magnesiothermically Formed Porous Silicon Thin

Films on Silicon-on-Insulator Optical Microresonators for High-Sensitivity Detection." *Advanced Optical Materials* 2, no. 3 (2014): 235-239.

3. Shams Mousavi, Hamed, Farshid Ghasemi, Ali Asghar Eftekhar, and Ali Adibi. "Application of Lattice Plasmon Waves in a Bilayer Plasmonic Nanoantenna Array for Surface Enhanced Raman Spectroscopy." In *CLEO: QELS_Fundamental Science*, pp. FM4K-6. Optical Society of America, 2014.
4. Ghasemi, Farshid, Ali A. Eftekhar, Hamed Shams Mousavi, Reza Abbaspour, Hesam Moradinejad, and Ali Adibi. "Lab-on-chip Silicon Nitride Microring Sensor at Visible Wavelength Using Glycoprotein Receptors." In *CLEO: Applications and Technology*, pp. AW1L-3. Optical Society of America, 2014.
5. Ghasemi, Farshid, and Ali Adibi, "An Accurate Interferometric Referencing Method for Resonance Tracking in Lab-on-chip Applications." In *CLEO: Science and Innovations*, pp. STh4H-4. Optical Society of America, 2014.
6. Ghasemi, F., M. Chamanzar, E. S. Hosseini, A. A. Eftekhar, Qing Li, A. H. Atabaki, and A. Adibi. "Compact fluorescence sensor using on-chip silicon nitride microdisk." In *Photonics Conference (PHO), 2011 IEEE*, pp. 151-152. IEEE, 2011.
7. Xia, Zhixuan, Ali Asghar Eftekhar, S. C. Davis, Ken Sandhage, and Ali Adibi. "Novel porous silicon integrated optical devices for sensing applications." In*Photonics Conference (PHO), 2011 IEEE*, pp. 545-546. IEEE, 2011.
8. Xia, Zhixuan, Ali Asghar Eftekhar, David Gottfried, Qing Li, and Ali Adibi. "Compact On-chip Multiplexed Photonic Gas Sensors." In *CLEO: Science and Innovations*, pp. JW2A-74. Optical Society of America, 2013.
9. Xia, Zhixuan, Ali Asghar Eftekhar, Qing Li, and Ali Adibi. "On-chip Multiplexed Photonic Gas Sensing for the Detection of Volatile Organic Compounds." In*Photonics Conference (IPC), 2012 IEEE*, pp. 548-549. IEEE, 2012.
10. Eftekhar, Ali A., Zhixuan Xia, Farshid Ghasemi, and Ali Adibi. "Ultra-Compact Multiplexed Lab-on-Chip Sensors using Miniaturized Integrated Photonic Resonators." In *Photonics Conference (IPC), 2012 IEEE*, pp. 439-440. IEEE, 2012.
11. F. Ghasemi, M. Chamanzar, A. A. Eftekhar, A. Adibi, "An interferometric referencing technique for wavelength noise reduction in biochemical sensing using on-chip cavities" Submitted to Lab on a Chip.
12. F. Ghasemi, A. Adibi, "On Resonance Detection Uncertainty in Presence of Additive Noise in Highly Multiplexed and Real-Time Tracking Systems," To be submitted to Analyst.
13. F. Ghasemir, A. A. Eftekhar, A. Adibi, "Spectrally/Spatially Multiplexed toxin detection using silicon nitride microring resonators at visible wavelength," to be submitted to Optics express
14. F. Ghasemi et al, "Multiplexed on-chip biosensor using silicon nitride microring resonator at visible wavelength for measurement of toxin detection using continuous-flow ion preconcentrator," To be submitted to Lab on the chip.

References:

[1] ACS. 2009. Cancer Facts and Figures 2009. American Cancer Society

[2] Hakomori, S. 1989. Aberrant glycosylation in tumors and tumor-associated carbohydrate antigens Adv. Cancer Res. 52:257-331

[3] Jun Hirabayashi, Atsushi Kuno, Hiroaki Tateno "Lectin-based structural glycomics: A practical approach to complex glycans" ELECTROPHORESIS. May 2011, Vol. 32, No. 10: 1118-1128

[4] De Vos, K.; Girones, J.; Popelka, S.; Schacht, E.; Baets, R.; Bienstman, P. "SOI optical microring resonator with poly(ethylene glycol) polymer brush for label-free biosensor applications." Biosens. Bioelectron. 2009, 24, 2528-2533

[5] H. Chang, F. Ishikawa, R. Zhang, R. Datar, R. Cote, M. Thompson, C. Zhou, "Rapid, Label-Free, Electrical Whole Blood Bioassay Based on Nanobiosensor Systems" ACS Nano. 2011 Dec 27;5(12):9883-91.

[6] Buchwalow, I., Samoilova, V., Boecker, W. & Tiemann, M. Non-specific binding of antibodies in immunohistochemistry: fallacies and facts. Sci. Rep. 1, 28; DOI:10.1038/srep00028 (2011)

[7] http://www.nanocs.com/PEG/SFPEG.htm

[8] M. Iqbal, et al., "Label-free biosensor arrays based on silicon ring resonators and high-speed optical scanning instrumenta-tion," IEEE STQE, 16 (3), pp. 654661, 2010.

[9] T. Lu, et al., "High sensitivity nanoparticle detection using optical microcavities," PNAS, 108 (15), pp. 59765979,(2011).

[10] F. Ghasemi, et al., "Self-referenced silicon nitride array microring biosensor for toxin detection using glycans at visible wavelength," in SPIE BiOS., 2013.

[11] Z Xia, AA Eftekhar, SC Davis, K Sandhage, A Adibi," Novel porous silicon integrated optical devices for sensing applications," IEEE Photon. Conf. (IPC), 2011, 545-546

[12] T.E.W. Niebe, J.P.M.Niederer, T. Gjervan, and W.F. Holderich, "Synthesis and characterisation of titanium-containing MCM-41 using (NH4)3[Ti(O2)F5] as the titanium source," Microporous Mesoporous Mater., 21, 67-74 (1998).

[13]K. Du, D. Yang, and Y. Sun, "Controlled fabrication of porous titania beads by a sol–gel templating method," Ind. Eng. Chem. Res., 48,755–762 (2009).

[14] I. Rendina, I. Rea, L. Rotiroti, and L. De Stefano, "Porous silicon-based optical biosensors and biochips," Physica E 38, 188-192 (2007).

[15] H. Ouyang, M. Christophersen, R. Viard, B. L. Miller, and P. M. Fauchet, "Macroporous silicon microcavities for macromolecule detection," Adv. Funct. Mater. 15, 1851-1859 (2005).

[16] H. Ouyang, C. C. Striemer, and P. M. Fauchet, "Quantitative analysis of the sensitivity of porous silicon optical biosensors" Appled Physics Letters, 88, 163108, 2006

[17] Belanger, A., et al., Molecular mass and carbohydrate structure of prostate specific antigen: studies for establishment of an international PSA standard. Prostate, 1995. 27(4): p. 187-97.

[18]Armbruster, D.A., Prostate-specific antigen: biochemistry, analytical methods, and clinical application. Clin Chem, 1993. **39**(2): p. 181-95.

[19]White, K.Y., et al., Glycomic characterization of prostate-specific antigen and prostatic acid phosphatase in prostate cancer and benign disease seminal plasma fluids. J Proteome Res, 2009. **8**(2): p. 620-30.

[20] Peracaula, R., et al., Altered glycosylation pattern allows the distinction between prostate-specific antigen (PSA) from normal and tumor origins. Glycobiology, 2003. **13**(6): p. 457-70.

[21] Prakash, S. and P.W. Robbins, Glycotyping of prostate specific antigen. Glycobiology, 2000. **10**(2): p. 173-6.

[22] Okada, T., et al., Structural characteristics of the N-glycans of two isoforms of prostate-specific antigens purified from human seminal fluid. Biochim Biophys Acta, 2001. **1525**(1-2): p. 149-60.

[23] Tabares, G., et al., Free PSA forms in prostatic tissue and sera of prostate cancer patients: analysis by 2-DE and western blotting of immunopurified samples. Clin Biochem, 2007. **40**(5-6): p. 343-50.

[24] Tabares, G., et al., Different glycan structures in prostate-specific antigen from prostate cancer sera in relation to seminal plasma PSA. Glycobiology, 2006. **16**(2): p. 132-45.
[25]Saldova, R., et al., Core fucosylation and alpha2-3 sialylation in serum N-glycome is significantly increased in prostate cancer comparing to benign prostate hyperplasia. Glycobiology, 2011. **21**(2): p. 195-205.
[26]Sarrats, A., et al., Glycan characterization of PSA 2-DE subforms from serum and seminal plasma. OMICS, 2010. **14**(4): p. 465-74.
[27] Glycobiology 16(2):132-145;
[28] Ohyama et al (2004)
[29] Glycobiology 14(8):671-9
[30]Vermassen et al (2012) Clin Chim Acta 413(19-20):1500-5